Eco. Env. & Cons. 29 (August Suppl. Issue) : 2023; pp. (S434-S440)
Copyright@ EM International
ISSN 0971–765X

DOI No.: http://doi.org/10.53550/EEC.2023.v29i04s.067

Biosynthesis of nickel oxide nanoparticles using *Delonixelata* extract for anticancer activity

V. Shanmugapriya[1] and S. Suguna[1]

[1]Photocatalysis Laboratory, Department of Chemistry, M.R. Govt. Arts College, Mannargudi 614 001, (Affiliated to Bharathidasan University 620 024), Tamil Nadu, India

(Received 4 April, 2023; Accepted 17 June, 2023)

ABSTRACT

Biosynthesis of nanoparticles has recently gained the attention of scientists because of the necessity to discover new techniques of synthesis that are safe, cost-effective and dependable. In a wide range of applications, metal oxide nanoparticles are increasingly gaining interest in particular. In this research, we produced NiO nanoparticles by green technology utilising Delonixelata extract, a natural non-toxic hydrocolloid and explored its potential antibacterial, anticancer and antioxidant use. The biosynthesized nickel oxide nanoparticles (NiO) were studied by Scanning electron microscopy (SEM), X-ray diffraction (XRD), and UV-visible spectroscopy. The findings revealed that NiO nanoparticles produced from Delonixelata exhibited better anticancer activity against renal cancer cell line (ACHN). An in vitro cell assay showed that NiO nanoparticles were significantly cytotoxic against the renal cancer cell line (ACHN).

Key words: *Delonixelata, Biosynthesis nanoparticle, Nickel oxide, Anticancer activity*

Introduction

Nanotechnology is one of the most important and rapidly increasing areas in the realm of science and engineering. It combines the knowledge of chemistry, biology, materials science, and other related fields of study to create new technologies. The word "nano" originates from a Greek language and means "dwarf" or "very little." Its dimensions range from 1 to 100 nanometers (nm). Because of their very little size, nanoparticles have a surface-to-volume ratio that is exceptionally high. Nanoparticles are sometimes known as Nano-crystals. Nanoparticles are classified into a wide variety of shapes, including nanocube, nanoflower, nanotube, and nanowire (Khatami *et al*., 2018). Nanoparticles are classified into many categories according to their structures, such as clusters, core shells, bimetallic, and so on (Karthik *et al*., 2018). Nanoparticles have a broad variety of uses in a variety of various commercial fields, including food, cosmetics, agriculture, medication delivery, cancer detection and diagnostics, cancer treatment, and many more fields (Iqbal, *et al*., 2018). The wide variety of uses for nanoparticles may be attributed to their interesting and one-of-a-kind features (magnetic, optical, chemical, electronic, mechanical, and sensing properties). Metallic nanoparticles, also known as MNPs, have several characteristics that are notably different from those of their bulk materials (Han, *et al*., 2017). These qualities include size, shape, surface effect, electrical and magnetic properties (Mayedwa, *et al*., 2018).

Despite the fact that nature has a great number of metal nanoparticles and metal oxide nanoparticles, including silver, platinum, gold, copper, magnesium, cobalt, caesium oxide, zinc oxide, etc. (Yang, *et al*., 2018). The scientific community's attention has

been drawn to NiO nanoparticles in particular among the many MNPs owing to the fact that they are both multifunctional and modifiable. NiO nanoparticles are one of the most engineered nanoparticles; they have an average size of 34 nm, a broadband gap that ranges from 3.7 to 40 eV, and they are an inherent p-type semiconductor. NiO nanoparticles have a broad variety of uses, including electrochromic test devices, lithium-ion batteries, supercapacitors, smart windows, water purification by photocatalysis, electrochemical sensors, and catalysis of chemical processes (Sone *et al*., 2016). In addition, NiO nanoparticles have potential uses in the adsorption of hazardous colours and contaminants in the environment (Khalil *et al*., 2018). Because of their ability to reduce inflammation, nanoparticles of NiO have potential applications in the field of biomedicine (Pandian *et al*., 2015). The previous study on NiO nanoparticles has shown that they have cytotoxic effects. These effects are caused by the release of ROS and Ni^{++}, which leads to oxidative damage (Sudhasree *et al.,* 2014). Sol-gel, galvanostatic anodization (Gong *et al*., 2015), electrodeposition (Zhang, 2015), hydrothermal (Kundu and Liu, 2015), solvothermal (Soomro *et al*., 2015), and co-precipitation are some of the physical and chemical methods that may be used to produce NiO nanoparticles. However, these physicochemical techniques have a large number of potentially hazardous adverse effects, which restricts the breadth of the biological applications that may be accomplished effectively (Thema *et al*., 2016). Synthesis through physical means requires large amounts of energy input, while chemical synthesis almost always results in the generation of hazardous chemical waste that contributes to environmental toxicity and produces items that cannot be degraded (Thovhogi *et al.,* 2015).

In recent years, it has been possible to accomplish green synthesis of NiO nanoparticles, and there is an increasing interest in the synthesis of NiO nanoparticles for various biological purposes from several other medicinal plants. *Moringa oleifera* (Lam.) (Thema *et al*., 2015), *Agathosmabetulina* (Berg.), *Callistemon viminalis* (Sims.), *Tamarix serotine* (Bunge. ex Boiss.) (Ezhilarasi *et al*., 2016) and *Nephelium lappaceum* (L.) (Nasseri, 2016) have all had plant-mediated production of NiO nanoparticles described for species. In this work, we reported the synthesis of NiO nanoparticles utilising aqueous extracts of the leaves of *Delonixelata (*Yuvakkumar, *et al*., 2014). No surfactant or organic/inorganic solvents were used in the process (Ovais, 2018). In addition, the characteristics of green NiO nanoparticles were determined by utilising UV, XRD, HRTEM, and FTIR. In addition, a variety of in vitro cytotoxicity tests are being performed on ACHN cancer cell lines.

Materials and Methods

Materials

All of the chemicals, solvents, and dyes used in the experiment were of the highest grade and were purchased in India from Merck (Pvt.) Ltd.

Preparation of plant extract

30 g of cleaned, dried *Delonixelata* leaf powder was added to 300 ml of deionized water, mixed with a magnetic stirrer, and then placed on a hot plate at 80 ^{0}C for two hours. After allowing the plant extract to come to room temperature, it was filtered three times using Whatman filter paper in order to achieve an aqueous extract that was completely free of impurities. When brought back to room temperature, the aqueous extract had a pH that was tested to be 7.3, which is considered to be neutral. In order to get the plant extract ready for use in subsequent studies, it was kept in the refrigerator at a temperature of 4 ^{o}C.

Synthesis of NiO nanoparticles

In order to initiate the production of NiO nanoparticles, the leaf extract of *Delonixelata* and nickel nitrate (Merck Chemicals, India, 99% purity) were used as precursors in the hot plate combustion process. 80 millilitres of an aqueous solution that included 0.1 millilitres of nickel nitrate was mixed with 20 millilitres of plant extract and agitated continuously for one hour. The end result was a solution that was completely transparent and uniform throughout. After 15 minutes of heating on a hot plate heater at a temperature of 250 ^{o}C, the resulting homogenous solution was ready for use. After the solution was boiled, dehydrated, broken down, and gas evolved, a black powder was produced. This powder was then dried in an oven with heated air at a temperature of 110 ^{o}C. In the end, the brown powdered NiO nanoparticles were annealed at a temperature of 300 ^{o}C for two hours, which produced 1.5 g of nickel oxide by weight.

Characterization of NiO nanoparticles

An HRTEM was used in order to investigate the morphology of the produced NiO nanoparticles (JEOL Japan, JEM-2100 plus). From HRTEM pictures, random diameter measurements of nanoparticles were taken with the use of the Image J imaging programme. At a wavelength ranging from 350 to 500 nm, a UV-vis spectrophotometer made by Perkin Elmer called the Lambda-35 was used to do an analysis of the NiO nanoparticles that were artificially produced. An X-Ray Diffractometer was used at 0.15405 Å with Cu-K in the Braggs angle range 2 to investigate the physicochemical properties of the NiO nanoparticles (10-80p). FTIR (Fourier transform infrared) spectroscopic analysis (FTIR, Agilent technologies) with KBr pellet in the range 4000-400 cm^{-1} was used to elucidate the functional groups and chemical compositions of the synthesised NiO nanoparticles. This was done in order to better understand the properties of the nanoparticles.

Anticancer activity of NiO nanoparticles

The cytotoxicity of green synthesis NiO nanoparticles against ACHN cell lines from patients with lung cancer. The National Centre for Cell Science in Pune, India, has obtained cell lines via the use of procurement. The cell lines were kept at a 5 percent CO_2 concentration in an incubator containing CO_2 at 37 °C. Transferring cell lines onto 96-well plates was done at a concentration of 1 x 103 cells per well, and the plates were left to incubate for 24 hours. After that, the cells were starved for one hour at 37 °C in a CO_2 incubator while being rinsed with 100 microliters of serum-free media. Following this step, the cells were treated with varying concentrations of NiO nanoparticles (ranging from 5 to 100 g / ml) before being placed back into the CO_2 incubator for a further 24 hours. Aluminium foil was used to cover the 96-well plates that contained the cells so that they would not be exposed to light. After the first incubation period had ended, the MTT solutions, at a concentration of 0.05 mg/mL, were added to each well. The plates were then placed in an incubator containing CO_2 and heated to 37 degrees Celsius for another four hours. Following the incubation period, the MTT reagents were removed, and the cell lines were rinsed with 200 µl of phosphate buffer saline (PBS). One hundred microliters of DMSO were employed in order to dissolve the crystals. The absorbance value was measured at a wavelength of 570 nm. A graph was created by plotting the absorbance value versus the concentration of cell density. The experiment was done three times to ensure accuracy.

Results and Discussion

Morphological studies

According to the high-resolution transmission electron microscopy, the biosynthesized NiO nanoparticles were evenly dispersed and assumed a somewhat agglomerated and spherical shape (Figure 1). An example of a typical HRTEM image of NiO nanoparticles is shown in Figure 1. These nanoparticles have a clustering pattern that can be seen in the image. The formation of the cube-like and spherical shapes may be attributed to the significant quantity of heat that is generated during the combustion process. A low density, weak interparticle forces, and magnetic interactions between the particles may have all contributed to the formation of agglomeration. Other possible contributors include the heat produced during the combustion process and the subsequent generation of gas. The particle sizes shown in the HRTEM image were measured using Image J, and the distribution frequencies of each particle size were computed thereafter. As can be observed in the particle size distribution curve shown in Figure 1, the NiO nanoparticles displayed an extremely small diameter, which was around 13.2± 1.3 nm. The biosynthesized NiO nanoparticles have a small particle size, a large specific surface area, and high dispersity, all of which suggest that this nanoparticle might be a promising material for the research of anticancer studies.

FTIR

Figure 2 shows the results of using FT-IR transmission spectra to determine the functional group of NiO nanoparticles. These results may be seen here. The Ni-O vibration (stretching mode) is located in a

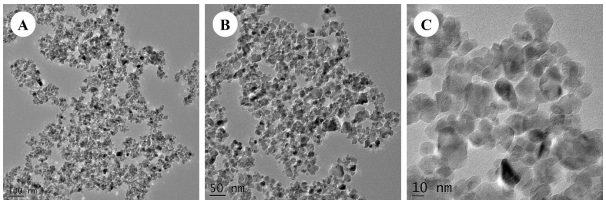

Fig. 1. HRTEM image of NiO nanoparticles

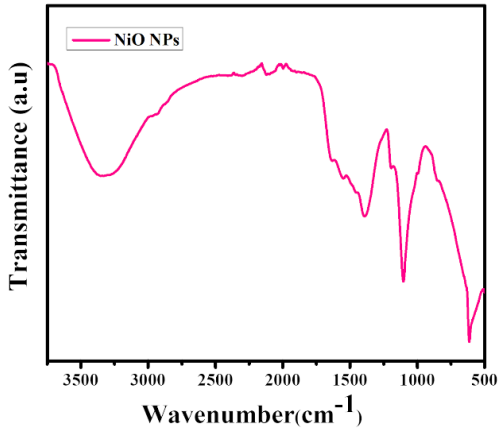

Fig. 2. FTIR spectra of NiO nanoparticles.

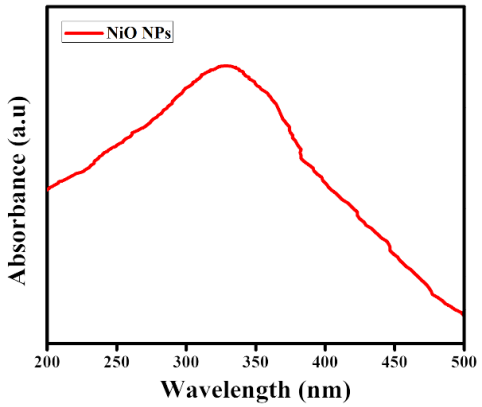

Fig. 3. UV-visible spectra of NiO nanoparticles.

wide range that may be found between 400 and 600 cm^{-1}. In the absorption spectra of inter-atomic vibrations, which are notably common in metal oxide, bands with wavelengths shorter than 600 cm^{-1} may sometimes be visible. These vibrations occur between atoms. It is believed that the wide absorption band that has a centred peak at 3223 cm^{-1} is caused by the O-H stretching vibration of the interlayer water molecules. This vibration occurs when the interlayer water molecules are adsorbed on the nickel oxide nanoparticles during the calcination process. Strong and narrow bands were observed at

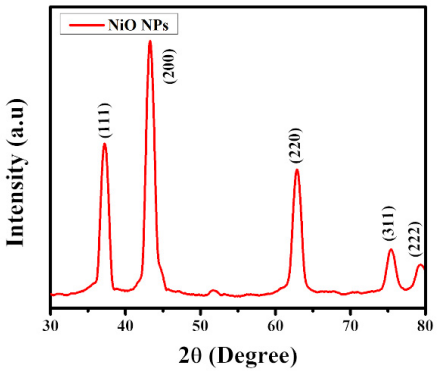

Fig. 4. XRD pattern of NiO nanoparticles.

1102 cm^{-1}, 1387 cm^{-1}, 1976 cm^{-1} and 1614 cm^{-1} due to the presence of a number of phytochemicals in the *Delonixelata* leaf extract. These bands correspond to the C-O stretching vibration, C=O stretching vibration of the acid group, para-substituted aromatic rings, and C=C aromatic stretching vibration mode. These bands were observed at 1100 cm^{-1}, 1384 cm^{-1}, 1970 cm^{-1}, and 1627 cm^{-1}.

UV-Visible spectroscopy

As can be seen in Figure 3, UV-Visible Spectroscopy was used to investigate the spectra of biosynthesized NiO nanoparticles between 300 and 800 nm in wavelength. The UV-visible spectra of NiO nanoparticles at 328 nm are the result of charge transfer from the conduction band (CB) to the valance band (VB) of the cations. The size of the particle can be seen to be diminishing as it travels closer to shorter wavelength signals in the spectrum. As a consequence of this, the synthesis of oxides between functional group bond formations was thought to be responsible for metal nucleation.

XRD

The XRD pattern of biosynthesized NiO nanoparticles derived from *Delonixelata* may be shown in Fig. 4. All of the peaks that were assigned

Table 1. Anticancer activity of NiO nanoparticles against renal cancer cell line (ACHN).

Concentration (µg/ml)	*Delonixelata*	Nickeloxide NPs	Cyclophosphamide
5	75.54±2.2	88.15±2.1	86.75±2.2
10	67.44±1.9	75.72±2.3	72.68±2.1
25	56.18±2.3	59.68±2.3	21.41±1.8
50	46.94±2.3	37.54±2.1	10.71±2.2
100	32.02±2.1	25.75±2.2	2.98±2.1

to the planes that were located at 36.92p, 42.63p, 63.97p, 73.51p, and 77.20p were well matched with JCPDS Card no.04–0835 with the FCC (Face centred cubic) crystalline Bunsenite structure of NiO nanoparticles. These structures were respectively indexed with (111), (200), (220), and (311), respectively. In order to compute the size of the nanoparticles, the Debye-Scherrer equation (1) was used. This equation may be written as

$$D = \frac{K\lambda}{\beta \cos\theta} \quad .. (1)$$

The average crystallite size of biosynthesized NiO nanoparticles was calculated to be 12 nm using the Debye-Scherrer formula, and the results of this calculation were presented in the previous sentence. Where k is the wavelength of the X-ray (1.54 Å) Cu Ka radiation, D is the crystallite size of the k-shape factor (0.9), h is the Bragg angle from 2h value of the intensity peak from the XRD pattern, and b is the full width at half maximum of the diffraction of the biosynthesized NiO nanoparticles.

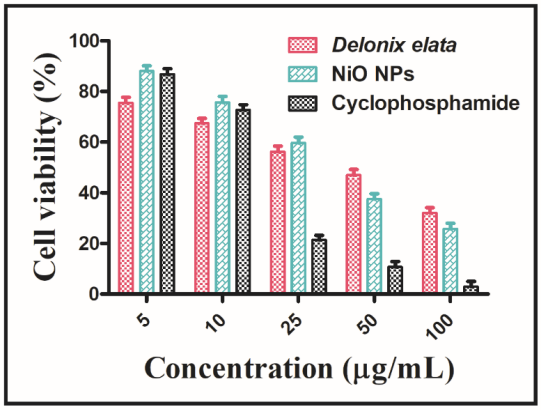

Anticancer activity

In vitro cytotoxicity activity against the ACHN cell line was investigated using the MTT test at varying doses of nickel oxide nanoparticles (NiO), *Delonixelata* extract, and cyclophosphamide served as the gold standard. Table 1 and Figure 5 demonstrate that cancer cell lines exposed to NiO nanoparticles had a dose-dependent decrease in their level of vitality. To investigate the impact that different concentrations of NiO nanoparticles have on anticancer activity by altering the concentrations from 5 µg, 10 µg, 25 µg, 50 µg, 100 µg, respectively. In spite of the high concentration of NiO nanoparticles, the anticancer activity was significantly enhanced. Therefore, the concentration of NiO nanoparticles is an extremely important factor in determining the efficacy of anticancer medications. The least concentration necessary to block the growth of cancer cell lines was determined to be 5 micrograms of NiO nanoparticles per cell. According to the research, the maximum inhibitory doses were found to be 100 µg and 50 µg. ACHN cancer cell therapies using NiO nanoparticles are more hazardous. In ACHN cancer cells, the doses of 50 µg and 100 µg per litre, respectively, were shown to be necessary for a cell death rate of fifty percent.

Conclusion

The extract of *Delonixelata* leaves was used as a starting material for the synthesis of nickel oxide nanoparticles. The peak of the UV–Visible absorption was measured to be 328 nanometers. The FTIR spectra of the synthesised nanoparticles exhibit peaks that are characteristic of functional groups such as O-H groups, N-H groups, C-N groups, and -C=O groups. According to the XRD pattern, the average crystal size of the nanoparticles is 12 nm when using the above equation to calculate it. The HRTEM image reveals that NiO nanoparticles have a spherical shape and are well-agglomerated, and their particle sizes range from 40 to 60 nanometers. Following the in vitro research described above, it is possible to draw the conclusion that NiO nanoparticles exhibit potent anticancer activity. It has been shown to have significant antimicrobial activity against pathogenic bacteria when present in high concentrations. It is an excellent source of compounds with anticancer capabilities.

References

Ezhilarasi, A.A., Vijaya, J.J., Kaviyarasu, K., Maaza, M., Ayeshamariam, A. and Kennedy, L.J. 2016. Green synthesis of NiO nanoparticles using Moringa oleifera extract and their biomedical applications: Cytotoxicity effect of nanoparticles against HT-29 cancer cells. *J. Photochem. Photobiol.* 164: 352.

Gong, N., Shao, K., Feng, W., Lin, Z., Liang, C. and Sun, Y. 2011. Biotoxicity of nickel oxide nanoparticles and bio-remediation by microalgae Chlorella vulgaris, *Chemosphere.* 83: 510.

Gong, N., Shao, K., Feng, W., Lin, Z., Liang, C. and Sun, Y. 2011. Biotoxicity of nickel oxide nanoparticles and bio-remediation by microalgae *Chlorella vulgaris. Chemosphere.* 83: 510.

Han, Y., Zhang, S., Shen, N., Li, D. and Li, X. 2017. Green synthesis and characterizations of Nickel oxide nanoparticles using leaf extract of Rhamnus virgata and their potential biological applications, *Mater.Lett.* 188: 1.

Iqbal, J., Abbasi, B.A., Ahmad, R., Mahmood, T., Ali, B., Khalil, A.T. and Munir, A. 2018 (b). Anomedicines for developing cancer nanotherapeutics: from benchtop to bedside and beyond. *Appl. Microbiol. Biotechnol.* 102 : 9449.

Karthik, K., Dhanuskodi, S., Gobinath, C., Prabukumar, S. and Sivaramakrishnan, S. 2018b. Fabrication of MgO nanostructures and its efficient photocatalytic, antibacterial and anticancer performance. *J. Mater Sci. Mater. Electron.* 7: 5459.

Kaviyarasu, K., Matinise, N. and Maaza, M. 2018. Green synthesis of nickel oxide, palladium and palladium oxide synthesized via Aspalathus linearis natural extracts: physical properties & mechanism of formation. *Appl. Surf. Sci.* 446: 266.

Khalil, A.T., Ovais, M., Ullah, I., Ali, M., Shinwari, Z.K., Hassan, D. and Maaza, M. 2018. Sageretia thea (Osbeck.) modulated biosynthesis of NiO nanoparticles and their in vitro pharmacognostic, antioxidant and cytotoxic potential. *Artif. Cells. Nanomed. Biotechnol.* 46 : 838.

Khalil, A.T., Ovais, M., Ullah, I., Ali, M., Shinwari, Z.K., Hassan, D. and Maaza, M. 2018. Sageretia thea (Osbeck.) modulated biosynthesis of NiO nanoparticles and their in vitro pharmacognostic, antioxidant and cytotoxic potential. *Artif. Cells. Nanomed. Biotechnol.* 46: 838.

Khatami, M., Alijani, H., Nejad, M. and Varma, R. 2018a. Core@shell Nanoparticles: Greener Synthesis Using Natural Plant Products, *Appl. Sci.* 8: 411.

Khatami, M., Varma, R.S., Zafarnia, N., Yaghoobi, H., Sarani, M. and Kumar, V.G. 2018e. Green synthesis of Nickel oxide nanoparticles. *Sustain. Chem. Pharm*. 10: 9.

Kundu, M. and Liu, L. 2015. Binder-free electrodes consisting of porous NiO nanofibers directly electrospun on nickel foam for high-rate supercapacitors. *Mater. Lett.* 144: 114.

Kundu, M. and Liu, L. 2015. Physical & Electrochemical Properties of Green Synthesized Bunsenite NiO Nanoparticles via, Callistemon iminalis' Extracts. *Mater. Lett.* 144: 114.

Mayedwa, N., Mongwaketsi, N., Khamlich, S., Kaviyarasu, K., Matinise, N. and Maaza, M. 2018. Green synthesis of nickel oxide, palladium and palladium oxide synthesized via Aspalathus linearis natural extracts: physical properties & mechanism of formation. *Appl. Surf. Sci.* 446: 266.

Nasseri, M.A. Ahrari, F. Zakerinasab, B. 2016. A green biosynthesis of NiO nanoparticles using aqueous extract of *Tamarix serotina* and their characterization and application. *Appl. Organomet Chem.* 30: 978.
of porous g-C3N4. *Appl Surf Sci.* 344: 33.

Ovais, M., Khalil, A.T., Raza, A., Islam, N.U., Ayaz, N.U., Saravanan, M. and Shinwari, Z.K. 2018. Phytochemical Analysis, Ephedra Procera C. A. Mey. Mediated Green Synthesis of Silver Nanoparticles, Their Cytotoxic and Antimicrobial Potentials. *Appl. Microbiol. Biotechnol.* 102: 4393.

Pandian, C., Palanivel, J. and Dhananasekaran, R.S. 2015. Green synthesis of nickel nanoparticles using *Ocimum sanctum* and their application in dye and pollutant adsorption, *Chin. J. Chem. Eng.* 23: 1307.

Pandian, C., Palanivel, J. and Dhananasekaran, R.S. 2015. Silver Nanoparticle Embedded á-Chitin Nanocomposite for Enhanced Antimicrobial and Mosquito Larvicidal Activity. *Chin. J. Chem. Eng.* 23: 1307.

Sone, B.T., Fuku, X.G. and Maaza, M. 2016. Physical & Electrochemical Properties of Green Synthesized Bunsenite NiO Nanoparticles via Callistemon Viminalis' Extracts, *Int J Electrochem Sci.* 11: 8204.

Sone, B.T., Fuku, X.G. and Maaza, M. 2016. Physical & Electrochemical Properties of Green Synthesized Bunsenite NiO Nanoparticles via Callistemon Viminalis' Extracts. *Int J Electrochem Sci.* 11: 8204.

Soomro, R.A., Ibupoto, Z.H., Abro, M.I. and Willander, M. 2015. Cobalt Oxide Nanoflowers for Electrochemical Determination of Glucose, *Sens. Actuator B-Chem.* 209: 966.

Sudhasree, S., Shakila Banu, A., Brindha, P. and Kurian, G.A. 2014. Synthesis of nickel nanoparticles by chemical and green route and their comparison in respect to biological effect and toxicity. *Toxicol Environ Chem.* 96: 743.

Sudhasree, S., Shakila Banu, A., Brindha, P. and Kurian, G.A. 2014. Synthesis of nickel nanoparticles by chemical and green route and their comparison in respect to biological effect and toxicity. *Toxicol Environ Chem.* 96: 743.

Thema, F.T. Manikandan, E. Gurib-Fakim, A. Maaza, M. 2016. Single phase Bunsenite NiO nanoparticles green synthesis by *Agathosma betulina* natural extract. *J Alloys Compd.* 657: 655.

Thema, F.T., Beukes, P., Gurib-Fakim, A. and Maaza, M. 2015. Green synthesis of Monteponite CdO nanoparticles by *Agathosma betulina* natural extract, *J Alloys Compd.* 646: 1043.

Thovhogi, N., Diallo, A., Gurib-Fakim, A. and Maaza, M. 2015. Nanoparticles green synthesis by *Hibiscus Sabdariffa* flower extract: Main physical properties. *J Alloys Comp.* 647 : 392.

Yang, Y., Zhang, W., Yang, F., Zhou, B., Zeng, D., Zhang, N., Zhao, G., Hao, S. and Zhang, X. 2018. Ru nanoparticles dispersed on magnetic yolk–shell nanoarchitectures with Fe3O4 core and sulfoacid-containing periodic mesoporous organosilica shell

as bifunctional catalysts for direct conversion of cellulose to isosorbide. *Nanoscale,* issue 5.

Yang, Y., Zhang, W., Yang, F., Zhou, B., Zeng, D., Zhang, N., Zhao, G., Hao, S. and Zhang, X. 2018. Ru nanoparticles dispersed on magnetic yolk–shell nanoarchitectures with Fe3O4 core and sulfoacid-containing periodic mesoporous organosilica shell as bifunctional catalysts for direct conversion of cellulose to isosorbide, Nanoscale,

Yuvakkumar, R., Suresh, J., Nathanael, A.J., Sundrarajan, M. and Hong, S.I. 2014. Novel green synthetic strategy to prepare ZnO nanocrystals using rambutan (*Nephelium lappaceum* L.) peel extract and its antibacterial applications. *Mater. Lett.* 128 : 170.

Zhang, Y. 2015. Isoelectric point and adsorption activity

Zhang, Y. 2015. Thermal oxidation fabrication of NiO film for optoelectronic devices. *Appl Surf Sci.* 344: 33.